



POLITECNICO DI TORINO  
Repository ISTITUZIONALE

Automatic localisation of innervation zones: a simulation study of the external anal sphincter

*Original*

Automatic localisation of innervation zones: a simulation study of the external anal sphincter / Mesin, Luca; Gazzoni, Marco; Merletti, Roberto. - In: JOURNAL OF ELECTROMYOGRAPHY AND KINESIOLOGY. - ISSN 1050-6411. - ELETTRONICO. - 19(2009), pp. e413-e421. [10.1016/j.jelekin.2009.02.002]

*Availability:*

This version is available at: 11583/2317484 since: 2021-08-21T18:30:06Z

*Publisher:*

Elsevier

*Published*

DOI:10.1016/j.jelekin.2009.02.002

*Terms of use:*

openAccess

This article is made available under terms and conditions as specified in the corresponding bibliographic description in the repository

*Publisher copyright*

Elsevier postprint/Author's Accepted Manuscript

© 2009. This manuscript version is made available under the CC-BY-NC-ND 4.0 license  
<http://creativecommons.org/licenses/by-nc-nd/4.0/>. The final authenticated version is available online at:  
<http://dx.doi.org/10.1016/j.jelekin.2009.02.002>

(Article begins on next page)

**AUTOMATIC LOCALISATION OF INNERVATION ZONES: A  
SIMULATION STUDY OF THE EXTERNAL ANAL SPHINCTER**

Luca Mesin, Marco Gazzoni, Roberto Merletti

Laboratorio di Ingegneria del Sistema Neuromuscolare (LISiN), Dipartimento di Elettronica,  
Politecnico di Torino, Torino, Italy

**Address for correspondence:**

Luca Mesin, Ph.D.

Dipartimento di Elettronica, Politecnico di Torino; Corso Duca degli Abruzzi 24, Torino, 10129 ITALY

Tel. 0039-011-4330476; Fax. 0039-0114330404; e-mail: [luca.mesin@polito.it](mailto:luca.mesin@polito.it)

## **ABSTRACT**

Traumas of the innervation zone (IZ) of the external anal sphincter (EAS), e.g. during delivery, can promote the development of faecal incontinence. Recently developed probes allow high-resolution detection of EMG signals from the EAS. The analysis of pelvic floor muscles by surface EMG (in particular, the estimation of the location of the IZ) has potential applications in diagnosis and investigation of the mechanisms of incontinence.

A method for the estimation of the IZ distribution of EAS from surface EMG is discussed and tested using an analytical model of generation of EMG signals from sphincter muscles. Simulations are performed varying length of the fibres, thickness of the mucosa, position of the motor units, and force level. Different distributions of IZ are simulated.

The performance is affected by surface MUAP amplitude (as the identification of IZ distribution by visual inspection). The performance is affected by mucosa thickness, decreases when fibre length is higher and reflects different MU distributions. However, in general the method is able to identify the position of two IZ locations and can measure asymmetry of the IZ distribution. This strengthens the potential applications of high density surface EMG in the prevention and investigation of incontinence.

**Keywords:** electromyography, innervation zone, sphincter muscle

## **1. INTRODUCTION**

Asymmetry of pelvic floor muscle innervation has been established in healthy subjects (Wietek et al., 2007). The properties of symmetry of the innervation zone (IZ) distribution in the external anal sphincter (EAS) have clinical relevance in case of pelvic floor trauma or incontinence surgery (Enck, 2004). Knowledge of the location of the IZ may help the surgeon in performing episiotomies with low risk of EAS partial denervation. The level of asymmetry has been proposed to be a predictor of increased risk for fecal incontinence in case of trauma (Enck, et al, 2004a; Wietek et al. 2007).

The neuronal control of the EAS in patients with defecation disorders is investigated in the clinical practice by invasive tools such as needle electromyography (EMG) (Enck, Hinninghofen et al, 2004a). The analysis of pelvic floor muscles by surface EMG has potential applications in diagnosis and investigation of the mechanisms of incontinence. Surface EMG has been detected non-invasively from sphincter muscles by either longitudinal or ring-shaped pairs of electrodes or perianal pairs of electrodes (Binnie et al., 1991; O'Donnell et al., 1988; Gee et al., 2000). High-resolution detection of surface EMG signal can be obtained by the use of recently developed probes, with a circular array of electrodes following the path of muscle fibres. With this technique, it is possible to identify the individual motor unit action potentials (MUAP) in the EMG signal, estimate the position of their IZ along the circumference, and follow the propagation of the action potentials along the muscle fibres (Enck et al., 2004b). Some preliminary studies based on multi-channel detection of surface EMG indicated anatomical differences between genders (Enck et al., 2004b; Enck et al., 2005), and assessed the correlation between childbirth-related sphincter injuries and faecal incontinence symptoms (Wietek et al., 2007).

The distribution of the IZ can be estimated by visual analysis of multi-channel surface EMG (Enck et al., 2004b) or by the application of an automatic method. This work is focused on

the validation and performance evaluation, on computer simulated EMG signals, of an automatic method for the estimation of the IZ distribution from surface EMG signals detected with a probe that carries a circumferential array of electrodes.

## **2. MATERIALS AND METHODS**

The location of the innervation zone (IZ) of a motor unit (MU) will be indicated by MUIZ and is defined as the centre of the region that includes the neuromuscular junctions of the MU fibres. In this work the expression “location of MUIZ” is also used to indicate the location where a MUAP initiates its bidirectional propagation. In both cases such a location is identified by an electrode number (Figure 1).

### *2.1 The algorithm for the estimation of the distribution of IZ*

The algorithm is based on the first step of the surface EMG decomposition method proposed by Gazzoni et al. (2004). The algorithm works on multi-channels EMG signals and is based on a segmentation-classification approach. The segmentation step extracts MUAPs from the multi-channel signals and it requires that the multi-channel detection system is approximately aligned with the fiber direction. The MUAP identification is performed by the Continuous Wavelet Transform (CWT), carried out on all channels. The application of the CWT to a signal can be interpreted as the application of a bank of filters with impulse responses which are scaled versions of a basic function, called mother wavelet (Chui, 1992). The use of the CWT is based on the observation that, because of the filtering effect of the volume conductor, the shape of MUAPs collected over the skin can be approximated as a dilated and attenuated version of a prototype waveform. The MUAP shape and consequently the selection of the mother wavelet mainly depends on the spatial filter used to detect signals (Farina et al., 2000; Merlo et al., 2003). Single differential (SD) spatial filter is used in this

work (not shown results indicate that the algorithm has equivalent performances using double differential filter).

The identification of candidate MUAPs consists in identifying the CWT maximum points in the two coordinates (scale and time). The time coordinate provides the temporal location of the candidate MUAP while the scale coordinate provides the information about the duration of the potential.

Once the time instants that are likely to correspond to the presence of MUAPs are identified for each channel, the a priori information on the propagation of the action potentials along the fibre is used to improve the segmentation procedure. A MUAP will appear in the EMG signal detected from a detection point with a delay proportional to the distance of the detection point from the IZ. The channel where the first CWT local maximum in time appears corresponds to the one nearest to the IZ.

Starting from the channel nearest to the IZ, the action potential should propagate along the channels following the circular path of the fibres. The delay in the detection of the same potential by adjacent detection points is estimated as the time shift that minimizes the mean square error, with a maximum likelihood criterion (Farina et al., 2003). The mean square error is computed in the time window which corresponds to the estimated duration of the candidate MUAP, given by the scale value of the maximum point of the CWT. The signals are aligned with the optimal delay and the correlation coefficients between the signal pairs in the identified window are estimated. The event detected is recognized as a MUAP on the basis of a threshold (0.7) on the average correlation coefficient. The algorithm is not able to solve superimposed MUAPs.

## *2.2 Simulated signals*

### *2.2.1 Model of simulation of single fibre potentials*

The generation model is based on the analytical solution for a cylindrical volume conductor (Farina et al., 2004). The model considers the generation of the intracellular action potentials at the end-plate, the propagation along the fibre, and the extinction at the fibre endings. These phenomena are described by the progressive appearing, propagation, and disappearing of the first derivative of the intracellular action potential, with intracellular action potential shape as proposed by Rosenfalck (1969).

The probe conductivity is neglected. The mucosa is infinite in the longitudinal direction, and placed between the probe and the muscle layer. The muscle is considered infinite in both the longitudinal and the radial direction (see Figure 1). The muscle layer accounts for both internal and external anal sphincter (IAS and EAS, respectively).

The conductivity of the mucosa is 1 S/m and the conductivity of the muscle is 0.5 S/m in the fibre direction and 0.1 S/m in the directions orthogonal to the fibre. The thickness of the mucosa layer is 1 or 3 mm, in two sets of simulations. The thickness of the IAS is 1 mm (Enck et al., 2005). This muscle is simulated by using the same conductivity as EAS, but no active fibres.

Two fibre angular lengths ( $180^\circ$  and  $230^\circ$ ) are considered (Figure 1a and 1b). The IZ is located under electrode 8 for all fibres (it will be moved to simulate different IZ distributions when the interference signals are created, see Section 2.2.3).

The detection system simulated is the probe described by Merletti et al. (2004) and is shown in Figure 1d. It consists in a cylinder, 14 mm in diameter, carrying a circular array of 16 silver bar electrodes (7x1 mm) equally spaced. Four anatomies were simulated corresponding to the combination of two mucosa thicknesses and two fibre lengths.

For each of the four simulated anatomies, 66 single fibre action potentials (SFAP) are simulated, generated by fibres with depth  $y_0$  in the range 1-6 mm and longitudinal distance  $z_0$  from the probe electrode ring in the range 0-5 mm (measured from the centre of the electrode).

### *2.2.2 Simulation of MUAP libraries*

Each library of SFAPs (corresponding to a specific anatomy, see Section 2.2.1) is used to build 10 MUAP libraries considering 10 different random distributions of sizes and locations of the MUs. The number of MU fibres is distributed as an exponential function with ratio of innervation numbers equal to 20 (Enoka and Fuglevand, 2001)). MU CV distribution is Gaussian (mean 4 m/s and standard deviation 0.3 m/s). Higher CV values are assigned to larger MUs. Each SFAP is used to simulate one MUAP (thus, each MUAP library contains 66 MUAPs), multiplying the SFAP by the number of fibres of the MU and approximating the smoothing due to the spread of the MUIZ and fibre endings (8 mm) by a time convolution with a Gaussian window function (with standard deviation given by

$$\sigma = \frac{4/3 \text{ mm}}{CV}, \text{ i.e. supposing that the Gaussian function has support within } \pm 3\sigma).$$

### *2.2.3 Simulation of IZ distributions*

To test the algorithm, two kinds of IZ distributions are simulated:

Simulation 1. In order to test the performance of the method in identifying the position of two IZs, a set of 6 distributions are simulated with one half of the MUs innervated under electrode 8 and one half of the MUs innervated under an other electrode ranging from 1 to 6. The 6 distributions are applied to each one of the 40 simulated MUAP libraries as described in the following.



Simulation 2. In order to test the performance of the method in estimating the asymmetry of the distribution of IZ, a set of 8 distributions is simulated with a Gaussian distribution of IZ centred in channel 8 and with a standard deviation ranging from 1 to 8 channels.

All MUAPs in the simulated libraries described in Section 2.2.2 have the innervation zone located under the electrode 8. To create the MU libraries with a specific distribution of IZ the following procedure is applied to each MUAP library:

- 1) Given a total number of 66 simulated MUs in a library, the number of MUs innervated under each electrode is evaluated from the desired distribution.
- 2) For each electrode, the MUs determined by point 1 are randomly chosen from the library without repetition. The MUIZ of these MUs is moved under the corresponding channel by shifting the MUAP signals.

The result is a set of 240 simulated libraries for Simulation 1 (4 anatomies, 10 MUAP libraries for each anatomy, 6 IZ distributions for each MUAP library) and 320 libraries for Simulation 2 (4 anatomies, 10 MUAP libraries for each anatomy, 8 IZ distributions for each MUAP library).

#### *2.2.4 Simulation of interference signals*

Signals (15 s long) recorded during isometric contractions at constant force are simulated. MUs are recruited according to the exponential function proposed by Fuglevand et al. (1993). At 75% MVC all MUs are recruited. The discharge statistics are modelled assuming minimum and maximum discharge rates of 8 and 35 pulses per second (pps), linear relation between force and discharge rate (0.5 pps/%MVC for all MUs), and Gaussian distribution of the interpulse interval variability with coefficient of variation 0.2. The MUs are recruited from low to high CV (Andreassen and Arendt-Nielsen, 1987).

Four contraction levels are considered: 20% MVC, 40% MVC, 60% MVC, and 80% MVC. Hence, for each of the 560 libraries described in Section 2.2.3 (240 corresponding to Simulation 1 and 320 to Simulation 2), 4 contraction levels are simulated, getting a total number of 2240 testing signals.

White Gaussian noise with 20 dB SNR is finally added to the simulated signals.

### 2.2.5 Distributions of IZ and performance indexes

The performance of the method is tested by comparing the estimated IZ distribution with two known distributions: the first considers the number of MUs innervated under each channel and is referred to as “numerical distribution”; the second is computed by weighting the “numerical distribution” by the surface EMG amplitude of the MUAPs and by the number of firings of the corresponding MUs in the interference signal and is referred to as “weighted distribution”. The “weighted distribution” is defined by assigning to each electrode the weight:  $\sum_{i \in MU\_IZ} pp_i nf_i$  where  $MU\_IZ$  is the set of MUs with IZ located under the considered electrode,  $pp_i$  is the peak to peak amplitude value of the MUAP belonging to MU  $i$ ,  $nf_i$  is the total number of firings of MU  $i$  in the 15 s long simulated interference signal.

Two different performance indexes are defined for Simulation 1 and Simulation 2 sets, described in Section 2.2.3.

Simulation 1. The performance of the method in resolving the position of two IZs is tested. The estimated distribution of IZ is modified by neglecting the channels under which less than 5% of the total number of identified MUAPs is found. A resolution of plus or minus one channel in the identification of the position of the IZ of a MUAP is accepted. For each channel  $ch$  corresponding to a simulated IZ, the percentage of MUAPs with IZ identified under channels  $\{ch-1 \ ch \ ch+1\}$  is estimated. In the case of IZ under channels 6 and 8, the

percentage of MUAPs with IZ identified under channel 7 is equally distributed between channel 6 and 8. In this way, the estimated distribution is substituted by two numbers indicating the percentage of IZs identified under each one of the two channels under which the two IZs were simulated.

The absolute value of the difference between the percentage of IZs identified under each of the two IZ channels and the simulated distributions (“numerical” and “weighted” distribution) are considered as the estimation error. Both the percentage of IZ identified far from the two channels of interest (separated by more than one channel distance) and the mistake in the estimation of the distribution of IZs in the correct positions contribute to the estimation error.

Simulation 2. The performance of the method in estimating the asymmetry of the distribution of IZ is tested. A percentage index of asymmetry is defined. The barycentre of the distribution of IZs is defined by considering the percentage number of IZs under a channel as a mass. The distance of the barycentre from the centre of the probe normalized with respect to the radius of the probe is considered as the asymmetry index. Thus, a symmetric distribution of IZs is associated to a vanishing value of asymmetry index. If the IZs of all MUs are under one single channel, the asymmetry index equals 1. The absolute difference between simulated and estimated asymmetry is considered as estimation error.

### *2.3 Statistical Analysis*

Analysis of variance (ANOVA) was applied on performance indexes (estimation error of IZ distribution and error in estimating asymmetry) to assess possible statistical dependence on the following 5 factors: MU distribution within the muscle, mucose thickness, fibre length, contraction level, distribution of IZ. Significance was set to  $p < 0.01$ .

### 3. RESULTS

Representative examples of simulated EMG signals are shown in Figure 2, for Simulation 1 and Simulation 2. The thickness of the mucosa is 1 mm, angular semilength of the fibres  $90^\circ$ , and force level 20% MVC. In A) and B), IZs are equally distributed under two electrodes (Simulation 1). In C) and D) IZs are distributed randomly, with Gaussian distribution (truncated on the circle and normalised) with standard deviation equal to 1 (C) or 8 (D) interelectrode distance (Simulation 2). The positions of some IZs identified by visual analysis of the signals are shown by a circle focusing the attention on the phase inversion of SD signals in the adjacent channels closest to the IZ.

An example of MUAPs identified in a simulated signal (Simulation 1) by the automatic method is shown in Figure 3. The detected MUAPs are highlighted and the small circles indicate the identified IZ positions.

Some examples of simulated and estimated IZ distribution are shown in Figure 4. Mucosa thickness is 1 mm, angular semilength of the fibres  $90^\circ$ , and force level 40% MVC. Portions of the simulated signals are shown. Both the “numerical distribution” (considering the number of MUs innervated under each electrode) and the “weighted distribution” (considering the amplitude and firing frequency of the MUAPs) are considered. IZs equally distributed under channel 4 and 8 (Simulation 1) are considered in A). It can be noticed from the portion of simulated signal shown in Figure 4A that the channels 5 to 12 are characterised by higher amplitude than the others. This is because, for the specific signal considered, recruited MUs innervated under electrode 8 have MUAPs with higher peak to peak amplitude than MUs innervated under electrode 4. Indeed, the “weighted distribution” shows a larger weight given to the IZ located under electrode 8 with respect to that located under electrode 4. Two representative examples of application of the method to signals correspondent to Gaussian distribution of IZ centred under electrode 8 with standard

deviation 1 and 8 electrodes, respectively (Simulation 2) are shown in B). The barycentre of the “numerical distribution” and of the “weighted distribution” are compared with the estimated one.

The results obtained in identifying the positions of two IZs (Simulation 1) are shown in Figure 5. Six different positions of the IZs (one IZ under electrode 8, the other under electrode 1, 2 ... 6) are considered. For each simulated “numerical distribution”, 10 different MU locations within the EAS are simulated (obtaining 10 different “weighted distributions”, as explained in Methods). A total number of 60 simulated signals (6 IZ locations by 10 MU distributions) are considered for each of 4 anatomies (thickness of mucosa 1 or 3 mm, angular semilength of the fibres 90° or 165°) and 4 force levels (20%, 40%, 60%, 80% MVC). Mean and standard deviation (across 60 simulated signals) of the errors are shown, for each anatomy and force level, both for the “numerical distribution” and the “weighted distribution”. ANOVA discloses that the performance of the method is affected by MU distribution (only in the case of “numerical distribution”), mucosa thickness (only in the case of “numerical distribution”, lower error for thicker mucosa), fibre length (lower error in the case of short fibres), and IZ distribution (small improvement in the case of closer locations of the two IZs). Contraction level does not affect the performance. The error in estimating the “weighted distribution” is significantly lower than that in estimating the “numerical distribution”. Signals 15 s long are processed, but the estimated IZ distribution did not undergo important changes after a few seconds. Hence, 1 – 2 second long signals are sufficient for the method to provide IZ distribution estimates.

The performance of the method in estimating asymmetry of IZ distribution (Simulation 2) is assessed in Figure 6. A force level of 80% MVC is considered in the figure (force level does not affect significantly the performance). Mean and standard deviation (across 10 simulated signals) of the absolute errors in estimating asymmetry are shown, for each of the 4

simulated anatomies (thickness of mucosa 1 or 3 mm, angular semilength of the fibres 90° or 165°), both for the “numerical distribution” and the “weighted distribution”. The performance of the method is affected by MU distribution (only in the case of “numerical distribution”), fibre length (lower error in the case of short fibres), and IZ distribution (equivalent results in estimating “numerical distribution” and “weighted distribution” for concentrated IZs, for more diffused IZ distribution decreasing/increasing performance in estimating the “numerical distribution”/ “weighted distribution”). Contraction level and mucosa thickness do not affect the performance. The error in estimating the “weighted distribution” is significantly lower than that in estimating the “numerical distribution”.

#### **4. DISCUSSION**

Non invasive assessment of IZ distribution of sphincter muscle has potential application in the prevention of sphincter problems due to episiotomy resulting in lesions of the EAS muscle. A method for the automatic estimation of IZ distribution in EAS is proposed. The method is based on the identification of single MUAPs and their IZ from EMG signals recorded with an array of 16 electrodes equally spaced along the circular path of the muscle fibres. The algorithm is applied to SD signals and the IZ is identified in correspondence of one SD channels. It is worth noticing that the detection point of a SD channel does not coincide with the position of an electrode (it is half way between two electrodes). Nevertheless, the angular distance between the location of the  $i^{\text{th}}$  electrode and the detection point of the  $i^{\text{th}}$  SD channel (about 11° for the simulated probe, Figure 1d) can be neglected for the purposes of this work.

The application to simulated signals indicates that the method can identify distinct IZ locations, with an average error of the order of 30% in the estimation of the “numerical

distribution” of IZ and of the order of 10% in the estimation of the “weighted distribution” (see Section 2.2.5 for the definition of “numerical” and “weighted” distribution).

The performance of the method depends on the reference IZ distribution considered. Estimation of “numerical distribution” is affected by mucosa thickness, with improving performance in the case of thicker mucosa. When mucosa is thinner, the detection is more selective and the method is sensitive to a low number of MUs. This decreases performance. Nevertheless, we cannot conclude that in general IZ “numerical distribution” can be better estimated in the case of thicker mucosa, as the amplitude of surface EMG signal is inversely related to mucosa thickness, and hence SNR (kept fixed in this simulation study) is expected to decrease in the case of thicker mucosa. Estimation of “numerical distribution” is affected by different distributions of the MUs within the muscle, as the method is sensitive to location and size of the MUs. The estimation of the “weighted distribution” is not affected by mucosa thickness and MU distribution (as peak to peak amplitude is affected by both factors).

Both the estimations of “numerical distribution” and “weighted distribution” are affected by fibre length. Indeed, longer fibres determine more interference between different MUAPs constituting the interference signal and cause larger errors. The estimations of “numerical distribution” and “weighted distribution” are also both affected by IZ distribution, with higher error in the case of more separated locations of the two simulated IZs. Indeed, crossings of propagating branches of different MUAPs are more likely in the case of more separated IZs and can determine wrong identifications of IZs that do not exist.

The algorithm can also compute an asymmetry index (defined in Section 2.2.5) of the IZ distribution, with absolute errors of the order of 20% considering the “numerical distribution” with higher errors in estimating more symmetric distributions, and of the order

of 10% considering the “weighted distribution” with higher errors in estimating more asymmetric distributions.

For a correct interpretation of the results it is necessary to consider the characteristics of the surface EMG. The detected signals are the summation of the MUAP trains of the active MUs. Two main factors must be taken into account in the evaluation of the method: A) the detection volume of the probe and B) the MUAP superpositions.

A) MUAPs belonging to MUs that are far from the electrodes do not significantly contribute to the signal and their IZ may go undetected.

B) The automatic method is not able to resolve superposition; for this reason, complex superimposed MUAPs may lead to the loss of identified IZs or to the identification of IZs that do not exist. However the results are not affected by the level of muscle activation when superpositions are more frequent than at lower levels. This indicates that the algorithm is not affected by MUAP superpositions.

Time support of a MUAP is of the order of 10 ms. It is reasonable to expect that no more than one MUAP every 10 ms can be detected either by visual inspection or by the proposed method (which is sensitive to the shape and amplitude of MUAPs, as visual inspection is). This means that the maximum number of detectable firings in one signal (15 s long) is of the order of 1-2 thousands (which is indeed the order of magnitude of the number of MUAPs identified by the method applied to a simulated signal). Considering the highest simulated force level (i.e. 80% MVC), all simulated MUs (i.e. 66 MUs) are recruited and most of them are firing at about 30 pps (close to the maximum simulated firing rate of 35 pps). This means that the total number of firings is about 2000 per second (and the maximum expected number of detected firings is 10 times lower). This also means that in a portion 10 ms long of a simulated signal (i.e., about the duration of a MUAP), about 20 MUs contribute to the signal. If one MUAP has much larger amplitude with respect to the others superimposed,



such a MUAP is the only one to be identified (either by visual inspection or by the proposed automatic method). If superimposed MUAPs have similar amplitudes, their contributions could be difficult to separate from the resulting interference signal, which can show large phase cancellations and shape variation across different channels. As a result, for the simulations considered, in the average, the number of identified firings is about 14%, 8%, 6%, 5% of the total for 20%, 40%, 60%, 80% MVC, respectively.

Thus, even assuming correct estimation of the position of the IZ of an identified MUAP, a large error could be expected in the determination of the IZ distribution, basically due to the limited number of MUs contributing to the surface EMG signal and the impossibility of identifying all their firings. As only a small percentage of the total number of firings can be expected to be identified, an estimation of IZ distribution can be obtained only in statistical sense. This means that we are trying to estimate the properties of a population of active MUs using data from the subpopulation of bigger or more superficial MUs. Only under the assumption that such a subpopulation is representative of the whole population we can make some inferences on the real IZ distribution, given the estimated one. In the simulated study here considered, the subpopulation of MUs which are identified by surface EMG could be considered as representative of the whole population of simulated MUs, as the sizes and locations of the MUs are randomly distributed but this may not be the case in real conditions. For example, if there is a correlation between IZ location and size of a MU, the estimation of the IZ distribution from surface EMG signal with the proposed method may be quite incorrect. Consider a case where two IZs are present, with all superficial and large MUs innervated under one electrode, and all deep and small MUs innervated under another electrode, our automatic method (as also visual inspection) could identify only the position of the first IZ. Nevertheless, the information about size is useful, as MUs with larger size can produce higher forces, thus being more important from a functional point of view. Hence,

the “weighted distribution” (which is estimated better than the “numerical distribution”) is biased by the size and firing rate of active MUs but may be more relevant in minimizing functional damage due to episotomy.

To improve the estimation of the “numerical distribution”, new probes with two dimensional systems of electrodes increasing the spatial sampling should be developed.

## **5. CONCLUSIONS**

A method for the estimation of IZ distribution in sphincter muscles is proposed. It is based on a matching filter algorithm. The performances of the algorithm are tested by changing IZ distribution, MU distribution in the muscle, fibre length, mucosa thickness, force level. The method is able to distinguish two IZ locations (separated by 1 channel) and can give indication on asymmetry of IZ distribution. The performance is affected by surface MUAP amplitude (so is the identification of IZ distribution by visual inspection), anatomy (mucosa thickness, fibre length) and MU distribution within the muscle. Nevertheless, the performance of the method is not affected by the level of contraction that is by the number and firing rate of the MUs. This result is important for practical application if we consider that, with the available probes, no feedback about the contraction level is provided. Furthermore, the method provides a reliable estimation of the IZ distribution within a few seconds. This makes the method feasible for the real time application in clinical settings.

The assessment of repeatability of the estimation of IZ distribution from experimental signals is the next step.

## **Acknowledgements**

This work was supported by project “Technologies for Anal Sphincters Analysis and Incontinence (TASI)” funded by Compagnia di San Paolo and Else Kroner-Fresenius-Stiftung and by project TIFNI.

## **REFERENCES**

Andreassen S, Arendt-Nielsen L. Muscle fiber conduction velocity in motor units of the human anterior tibial muscle: A new size principle parameter. *J. Physiol.*, 1987; 391: 561-571.

Binnie NR, Kawimbe BM, Papachrysostomou M, Clare N, Smith AN. The importance of the orientation of the electrode plates in recording the external anal sphincter EMG by non-invasive anal plug electrodes. *Int. J. Colorectal. Dis.*, 1991; 6: 5-8.

Chui K. *Wavelet Analysis and its Applications; volume 1: An Introduction to Wavelet*, Academic Press: San Diego, 1992.

Enck P, Hinninghofen H, Merletti R, Azpiroz F. The external anal sphincter and the role of surface electromyography. *Neurogastroenterol Motil.* 2005; 17 Suppl 1:60-7.

Enck P. Functional asymmetry of pelvic floor innervation--myth or fact? *Folia Med Cracov.* 2004; 45: 51-61. Review.

Enck P, Hinninghofen H, Wietek B, Becker HD. “Functional asymmetry of pelvic floor innervation and its role in the pathogenesis of fecal incontinence.” *Digestion.* 2004; 69: 102-11. 2004a. Review.

Enck P, Franz H, Azpiroz F, Fernandez-Fraga X, Hinninghofen H, Kaske-Bretag K, Bottin A, Martina S, Merletti R. Innervation zones of the external anal sphincter in healthy male and female subjects. Preliminary results. *Digestion.* 2004b; 69: 123-30.

Enoka RM, Fuglevand AJ. Motor unit physiology: some unresolved issues. *Muscle Nerve.* 2001; 24: 4-17, Review..

Farina D, Fortunato E, Merletti R. Non-invasive estimation of motor unit conduction velocity distribution using linear electrode arrays. *IEEE Trans. Biomed. Eng.* 2000; 41: 380-88.

Farina D, Mesin L, Martina S, Merletti R. A new surface EMG generation model with multi-layer cylindrical description of the volume conductor. *IEEE Trans. Biomed. Eng.* 2004; 51: 415-426.

Fuglevand AJ, Winter DA, Patla AE. Models of recruitment and rate coding organization in motor-unit pools. *J. Neurophysiol.* 1993; 70: 2470-88.

Gazzoni M, Farina D, Merletti R. A new method for the extraction and classification of single motor unit action potentials from surface EMG signals. *J. Neurosci. Methods.* 2004; 136: 165-77.

Gee AS, Jones RS, Durdey P. On-line quantitative analysis of surface electromyography of the pelvic floor in patients with faecal incontinence. *Br. J. Surg.* 2000; 87: 814-818.

Merletti R, Bottin A, Cescon C, Farina D, Gazzoni M, Martina S, Mesin L, Pozzo M, Rainoldi A, Enck P. Multichannel surface EMG for the non-invasive assessment of the anal sphincter muscle. *Digestion.* 2004; 69:112-22.

Merlo A, Farina D, Merletti R. A fast and reliable technique for muscle activity detection from surface EMG signals. *IEEE Trans. Biomed. Eng.*, 2003; 50: 316-23.

O'Donnell P, Beck C, Doyle R, Eubanks C. Surface electrodes in perineal electromyography. *Urology* 1988; 32: 375-379.

Rosenfalck P. Intra and extracellular fields of active nerve and muscle fibers. A physico-mathematical analysis of different models. *Acta Physiol. Scand.* 1969; 321: 1-49.

Wietek BM, Hinninghofen H, Jehle EC, Enck P, Franz HB. Asymmetric sphincter innervation is associated with fecal incontinence after anal sphincter trauma during childbirth. *Neurourol Urodyn.* 2007; 26: 134-9.

## FIGURE CAPTIONS

**Fig. 1** Cylindrical model of the volume conductor. The muscle extends to infinity in the radial direction and has longitudinal and transverse conductivity equal to 0.5 and 0.1 S/m, respectively. Mucosa has a conductivity of 1 S/m, and thickness 1 mm and 3 mm in different simulation sets. a) and b) Longitudinal sections for long and short fibres innervated under channel 1. c) Three dimensional view with the definition of the axial distance  $z_0$ . d) Anal sphincter probe, with one array of rectangular electrodes.

**Fig. 2** Examples of simulated SD EMG signals in the case of mucosa thickness 1 mm, angular semilength of the fibres  $90^\circ$ , force level 20% of MVC. a) and b) Simulation 1: IZ equally distributed under two electrodes. a) electrodes 2 and 8, b) electrodes 6 and 8. c) and d) Simulation 2: IZ with a Gaussian random distribution with standard deviations of c) 1 IED and d) 8 IED.

**Fig. 3** Example of MUAPs identification for a signal of the Simulation 1 set. The single differential signals are shown. The detected MUAPs are highlighted and circles indicate the identified IZ position. Simulation parameters: fiber angular semilength  $90^\circ$ , thickness of the mucosa layer 1 mm, position of the IZs - electrode 8 and electrode 4, contraction level 40% MVC.

**Fig. 4** Simulated and estimated IZ distribution in the case of mucosa thickness 1 mm, angular semilength of the fibres  $90^\circ$ , force level 40% MVC. Both the “numerical distribution” (considering the number of MUs innervated under each electrode) and the

“weighted distribution” (considering the amplitude and firing frequency of the MUAPs) are considered. A) Simulation 1: IZ equally distributed under channel 4 and 8. B) Simulation 2: Gaussian distribution of IZ centred under electrode 8 with standard deviation of 1 and 8 IEDs in two different simulations.

**Fig. 5** Assessment of the performance of the method in identifying the positions of two IZs (Simulation 1). Six different distributions of the IZs (one IZ under electrode 8, the other under electrode 1 to 6 in 6 simulations) are considered. For each simulated “numerical distribution”, 10 different MU locations within the EAS are simulated. A total number of 60 simulated signals (6 IZ locations by 10 MU distributions) are considered for each of 4 anatomies (thickness of mucosa 1 or 3 mm, angular semilength of the fibres  $90^\circ$  or  $165^\circ$ ) and 4 force levels (20%, 40%, 60%, 80% MVC). Mean and standard deviation (across 60 simulated signals) of the errors are shown, for each anatomy and force level, both for the “numerical distribution” and the “weighted distribution”.

**Fig. 6** Assessment of the performance of the method in identifying the asymmetry of the IZ distribution (Simulation 2). The asymmetry index is defined as the distance of the barycentre of the IZ distribution from the centre of the probe, normalised in order to range between 0 and 1. For each simulated “numerical distribution”, 10 different MU locations within the EAS are simulated (obtaining 10 different “weighted distribution”). Force level is 80%. Mean and standard deviation (across 10 simulated signals) of the absolute errors of the estimates of the simulated asymmetry are shown, for each of the 4 simulated anatomies (thickness of mucosa 1 or 3 mm, angular semilength of the fibres  $90^\circ$  or  $165^\circ$ ), both for the “numerical distribution” and the “weighted distribution”.

Figure 1

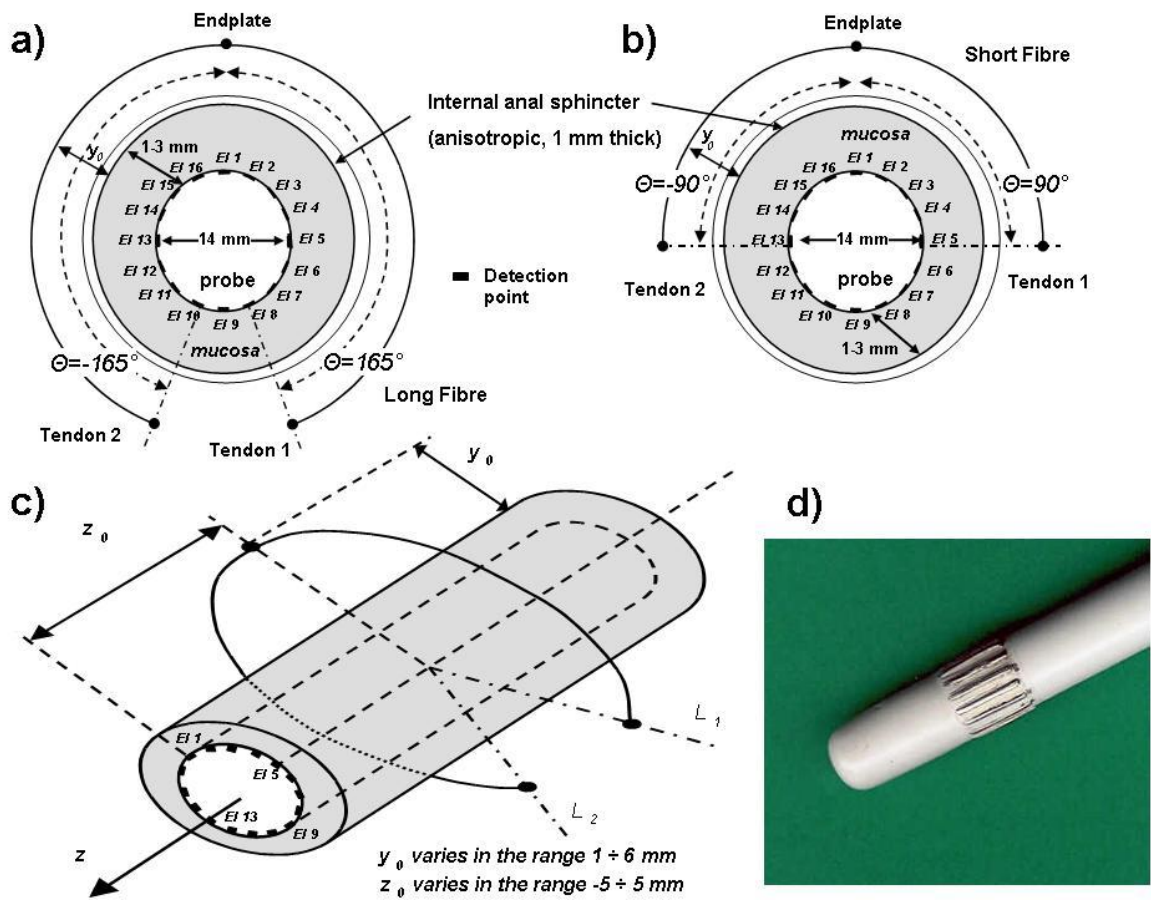


Figure 2

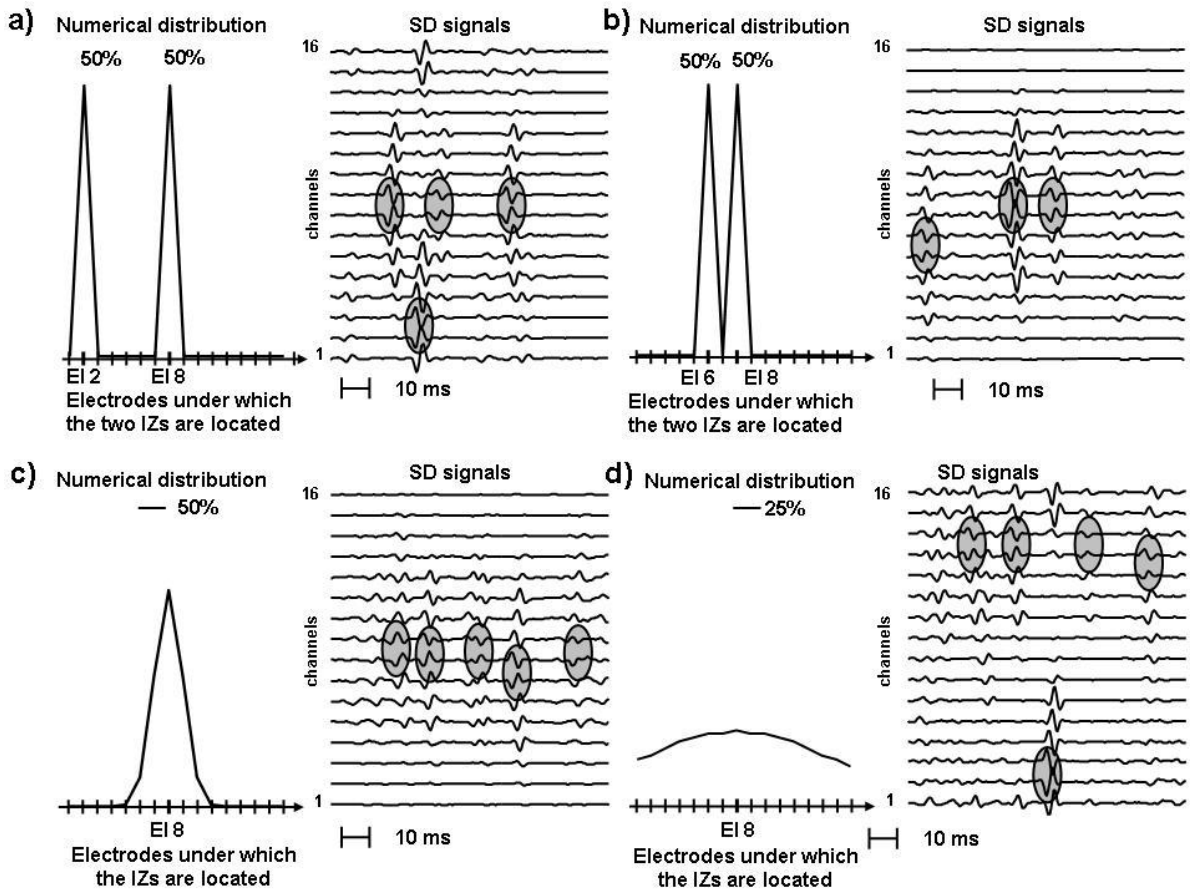




Figure 3

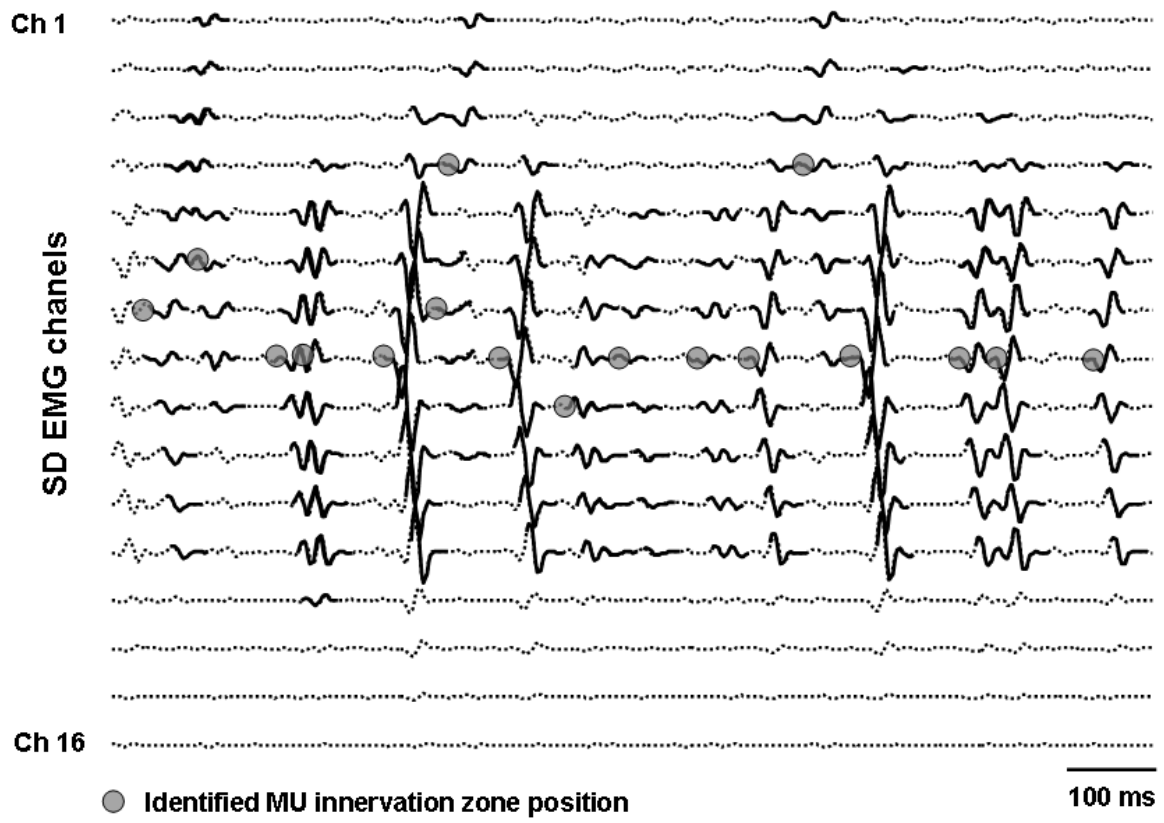


Figure 4

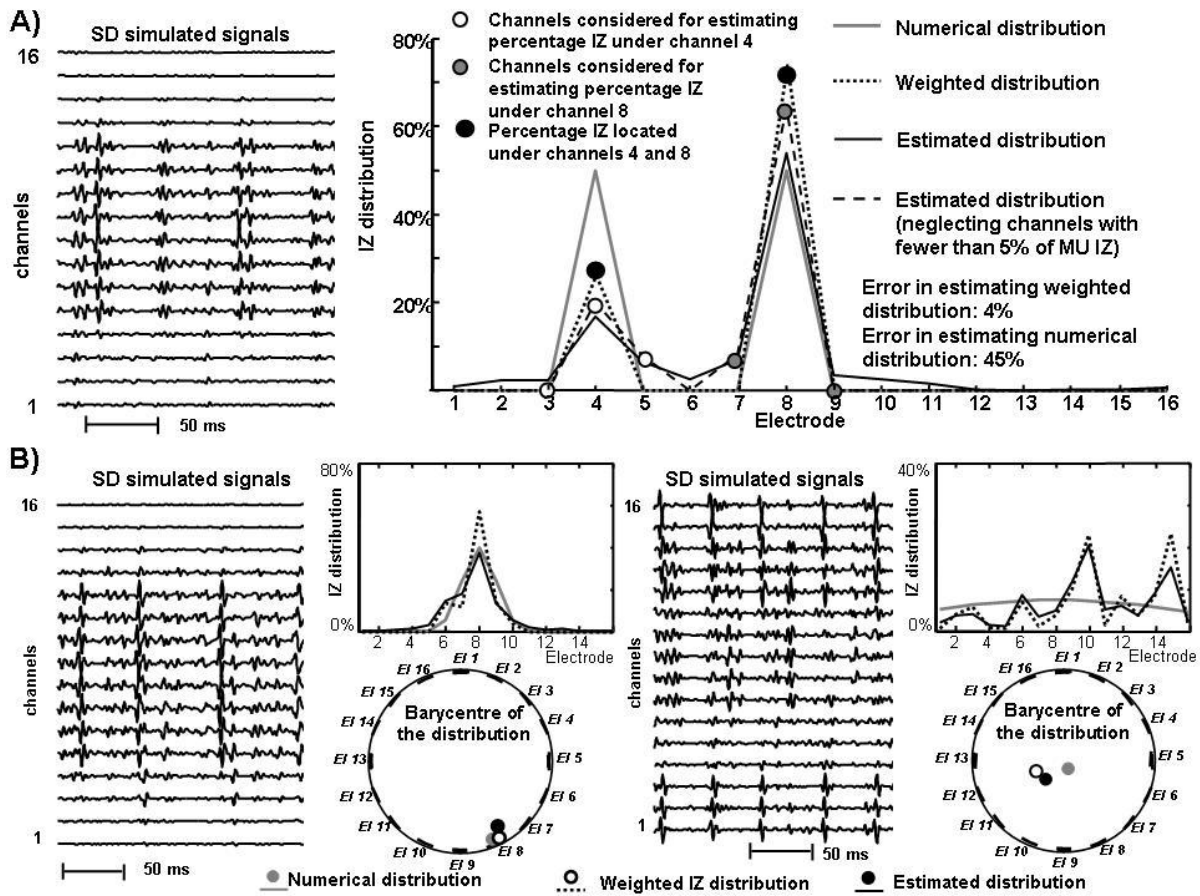


Figure 5

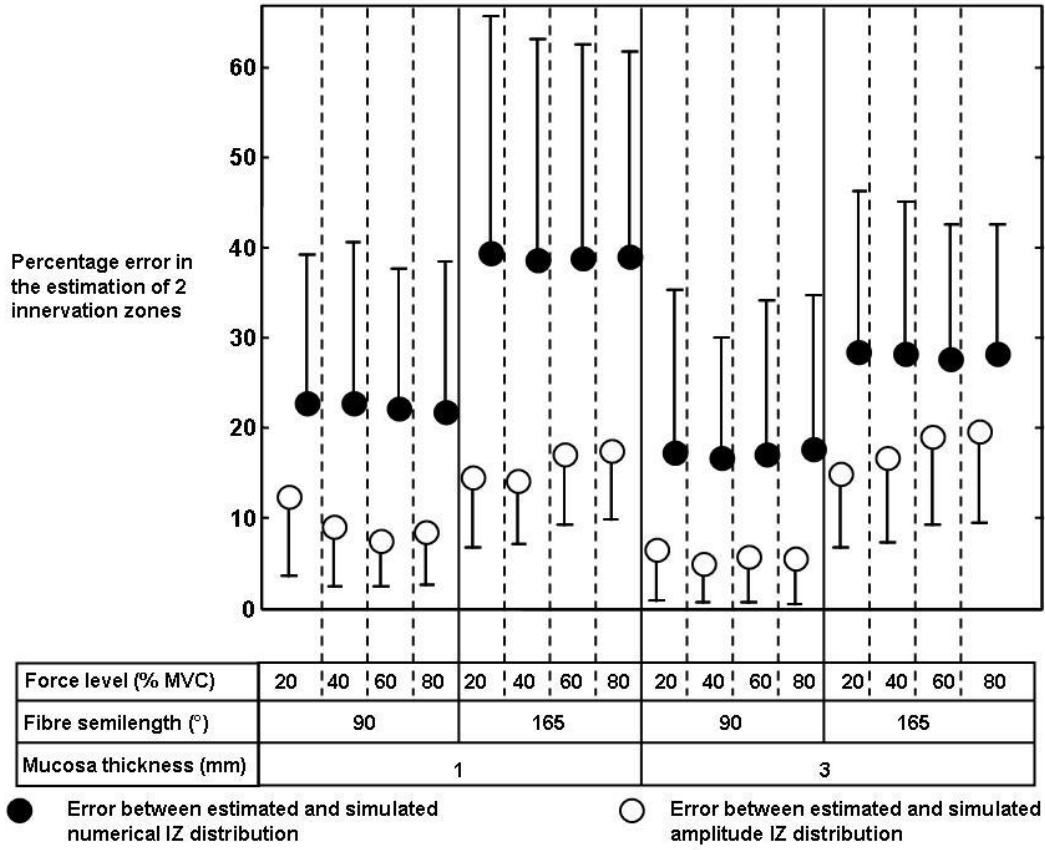


Figure 6

